REDUCED COMPLEXITY SINGLE-CARRIER MAXIMUM-LIKELIHOOD DETECTION FOR DECISION FEEDBACK ASSISTED SPACE-TIME EQUALIZATION

A. Wolfgang, J. Akhtman, S. Chen, L. Hanzo

School of ECS Univ. of Southampton, SO17 1BJ, UK.
Tel: +44-23-80-593 125, Fax: +44-23-80-594 508
{aw03r,yja02r,sqc,lh}@ecs.soton.ac.uk
http://www-mobile.ecs.soton.ac.uk

ABSTRACT

A novel Decision-Feedback (DF) aided reduced complexity Maximum Likelihood (ML) Space-Time Equalizer (STE) designed for single-carrier multiple antenna assisted receivers is introduced. The proposed receiver structure is based on a recursive tree search, which is capable of achieving ML performance at a moderate computational cost and substantially outperforms the linear benchmarker based on the Minimum Mean-Squared Error (MMSE) criterion. Additionally a further complexity reduction scheme is proposed, which exploits the specific characteristics of both the wide-band channel and the proposed DF-STE.

I. INTRODUCTION

In [1] a novel tree search based reduced complexity Maximum Likelihood (ML) detector designed for Orthogonal Frequency Division Multiplexing (OFDM) [2] systems has been introduced, which is referred to as the Optimized Hierarchical Recursive Search Algorithm (OHRSA). The OHRSA constitutes an evolution of the sphere decoder [3], which describes the system's transfer function using an upper triangular matrix and then detects the signal on a dimension by dimension basis. In contrast to conventional sphere decoding [3], the OHRSA retains its low complexity even in heavily overloaded systems, where the number of supported users is significantly higher than the number of receiver antennas. The computational complexity of the algorithm is close to that of the linear Minimum Mean Squared Error (MMSE) detector.

The first objective of this contribution is to employ the OHRSA in single-carrier synchronous uplink MIMO systems operating in a dispersive environment. Directly applying the OHRSA, which was originally designed for non-dispersive OFDM sub-channels in a wideband single-carrier system does have the potential of realizing a reduced complexity ML detector. However, employing the OHRSA in a wideband single-carrier environment involves the detection of undesired symbols engendered by the dispersive channel, which imposes an increased computational complexity. Therefore a low-complexity technique will be introduced for circumventing this problem in the context of single-carrier wideband systems.

The remainder of this paper is organized as follows. In Section II the basic system model describing the DF aided STE is introduced. The system model is used in Section III for introducing the basic concept of the OHRSA using a simple numerical example. Simulation results are provided in Section III-A for highlighting the potential performance improvements that may be achieved and the associated complexity is also discussed. In Section IV a modification of the standard OHRSA is proposed, which results in a further complexity reduction at a negligible performance degradation. Finally in Section V we offer our conclusions.

The financial support of the EU under the auspices of the Phoenix and Newcom projects and that of the EPSRC, UK is gratefully acknowledged. The authors are also grateful to their colleagues for the enlightenment gained within the Phoenix consortium.

II. SYSTEM MODEL

The system considered supports K number of perfectly synchronized Mobile Stations (MSs), each employing an N_{Tx}-element transmit antenna array and a Base Station (BS) receiver, which has N_{Rx} number of Antenna Elements (AEs). The MSs' transmitters channel encode the input bitstream, map the encoded bits to the N_{Tx} different transmit antennas and modulate the signal. The mapped symbols are transmitted to the BS over a frequency selective fading channel having a symbol-spaced Channel Impulse Response (CIR) characterized by the channel coefficients $h_{\jmath\imath,l}^{(k)}$.

The channel coefficient $h_{\jmath\imath,l}^{(k)}$ represents the complex-valued channel gain of the l^{th} multi-path component of the channel between the k^{th} MS's AE $\imath$ and the $\jmath^{th}$ BS receiver AE. Given the transmitted symbol $s_{\imath}^{(k)}(n)$, which is associated with the k^{th} MS's transmit AE $\imath$, the output signal of the $\jmath^{th}$ AE of the BS receiver at time instant n can be written as[1]

$$x_{\jmath}(n) = \sum_{k=1}^{K} \sum_{\imath=1}^{N_{Tx}} \sum_{l=1}^{L} h_{\jmath\imath,l}^{(k)} s_{\imath}^{(k)}(n-l-1) + \eta(n). \qquad (1)$$

Furthermore, L is the number of symbol-spaced multi-path components and $\eta(n)$ is the complex-valued Additive White Gaussian Noise (AWGN) having a variance of $E\left[|\eta_{\jmath}(n)|^2\right] = 2\sigma^2$.

Assuming that a MS transmits at a power of σ_k^2 and a channel code with rate R is used, the resultant E_b/N_0 is given as

$$\frac{E_b}{N_0} = \frac{\sigma_k^2 \sum_{\jmath=1}^{N_{Rx}} \sum_{\imath=1}^{N_{Tx}} \sum_{l=1}^{L} E\left[|h_{\jmath\imath,l}^{(k)}|^2\right]}{R \log_2(\mathcal{M}) N_{Tx} N_{Rx} 2\sigma^2}, \qquad (2)$$

where $\mathcal{M}$ is the number of modulation levels.

Under the assumption of perfectly synchronized transmitters the relation between the signal transmitted by the MSs' AEs and the channel's output for channel tap l is described by a $(N_{Rx} \times KN_{Tx})$-dimensional matrix $\boldsymbol{H}_l$, where the $(\jmath, (k-1)N_{Tx}+\imath)^{th}$ element of the matrix is given by $h_{\jmath\imath,l}^{(k)}$. For simplicity, let us denote the total number of transmitters in the system as $Q = KN_{Tx}$, with the associated transmitter index given by $q = (k-1)N_{Tx} + \imath$.

[1]Note, that the indices $\imath$ and $\jmath$ are associated with the transmit and receive AE respectively, whereas the indices i and j are used as running indices defined in the context where they occur.

1-4244-0270-0/06/$20.00 (c)2006 IEEE

This full text paper was peer reviewed at the direction of IEEE Communications Society subject matter experts for publication in the WCNC 2006 proceedings.

Considering a finite-length STE having a feed-forward order of M, the super-matrix $\mathbf{H}$, which represents the total system is obtained by concatenating the $(N_{Rx} \times Q)$-dimensional matrices $\boldsymbol{H}_l$, yielding:

$$\mathbf{H} = \begin{bmatrix} \boldsymbol{H}_1 & \cdots & \boldsymbol{H}_L & 0 & \cdots & 0 \\ 0 & \boldsymbol{H}_1 & \cdots & \boldsymbol{H}_L & \ddots & \vdots \\ \vdots & \ddots & \ddots & \ddots & \ddots & 0 \\ 0 & \cdots & 0 & \boldsymbol{H}_1 & \cdots & \boldsymbol{H}_L \end{bmatrix}.$$

Let us denote the N_{Rx}-element channel output vector as $\boldsymbol{x}(n)$. Then the channel output super-vector $\mathbf{x}(n) = [\boldsymbol{x}(n)^T \ldots \boldsymbol{x}(n - M + 1)^T]^T$ can be expressed as

$$\begin{aligned} \mathbf{x}(n) &= \mathbf{H}(n) \left[\boldsymbol{s}(n)^T, \ldots, \boldsymbol{s}(n - L - M + 2)^T\right]^T \\ &\quad + \left[\boldsymbol{\eta}(n)^T, \ldots, \boldsymbol{\eta}(n - M + 1)^T\right]^T \\ &= \mathbf{H}(n)\mathbf{s}(n) + \boldsymbol{\eta}(n) \\ &= \check{\mathbf{x}}(n) + \boldsymbol{\eta}(n), \end{aligned} \tag{3}$$

where $\boldsymbol{s}(n) = [s_1(n), \ldots, s_Q(n)]^T$ is a column vector containing the symbols transmitted by the $Q = KN_{Tx}$ AEs present in the system and $\boldsymbol{\eta}(n) = [\eta_1(n), \ldots \eta_{N_{Rx}}(n)]^T$. For notational simplicity the time-index n will be dropped, where this is possible without ambiguity. If referring to a delayed vector such as for example $\boldsymbol{s}(n - \Delta)$, this is indicated by $\boldsymbol{s}_{\Delta+1}$, which suggests that $\boldsymbol{s}_{\Delta+1}$ is the $(\Delta + 1)^{th}$ subvector of the super-vector $\mathbf{s}(n)$ defined in Equation (3).

The performance of both linear and non-linear equalizers can be enhanced by incorporating a decision feedback structure [4] in the receiver. In addition to the feed-forward order M and the decision delay [4] parameter of the STE we introduce the decision feedback order N. Note that the oldest symbol vector, which still influences the detected symbol $\hat{\boldsymbol{s}}_{\Delta+1}$ is $\boldsymbol{s}_{M+L}$. Furthermore, the oldest feedback symbol vector is $\boldsymbol{s}_{\Delta+N+1}$. Without loss of generality we therefore chose $N = M + L - 1 - \Delta$ for the characterization of the proposed Decision Feedback (DF) aided STE. In order to describe the feedback structure, we first partition the system matrix $\mathbf{H}$ into two sub-matrices [4] as follows:

$$\mathbf{H} = [\mathbf{H}_1 \ \mathbf{H}_2], \tag{4}$$

where $\mathbf{H}_1$ hosts the first $Q(\Delta+1)$ number of columns of $\mathbf{H}$, while $\mathbf{H}_2$ represents the last QN columns in $\mathbf{H}$. The array output can then be written as

$$\begin{aligned} \mathbf{x} &= \mathbf{x}_1 + \mathbf{x}_2 \\ &= \check{\mathbf{x}}_1 + \check{\mathbf{x}}_2 + \boldsymbol{\eta} \\ &= \mathbf{H}_1\mathbf{s}_1 + \mathbf{H}_2\mathbf{s}_2 + \boldsymbol{\eta}, \end{aligned} \tag{5}$$

where $\mathbf{s}_1 = \left[\boldsymbol{s}_1^T \ldots \boldsymbol{s}_{\Delta+1}^T\right]^T$ indicates the symbols in the feed-forward shift register and $\mathbf{s}_2 = \left[\boldsymbol{s}_{\Delta+2}^T \ldots \boldsymbol{s}_{\Delta+N+1}^T\right]^T$ denotes the symbols in the feedback register. The attainable complexity reduction and the achievable performance gain associated with DF is due to the fact that the previously received symbols of all transmitters have already been decided upon and hence their ambiguity imposed on the phasor constellation at the output of the dispersive channel may be eliminated.

Equation (5) may be interpreted as a space translation [5], where a received signal vector $\mathbf{x}$ is translated into the new observation space $\mathbf{r}$ by eliminating the phasor-points corresponding to the product of the DF sequence $\mathbf{s}_2$ and the channel matrix $\mathbf{H}_2$. The related space translation is described by

$$\mathbf{r} = \mathbf{x} - \mathbf{H}_2\mathbf{s}_2. \tag{6}$$

The DF assisted receiver first translates the received signal vector $\mathbf{x}$ into the translated space $\mathbf{r}$ and the detector then operates on the translated received signal vector $\mathbf{r}$ assuming that $\mathbf{H}_1$ was the observed channel matrix.

III. THE NEAR-ML DETECTOR

In this section the OHRSA approximate ML algorithm designed for the detection of the transmitted signal is highlighted [1]. For the sake of notational convenience we only consider a STE dispensing with DF. Its extension to a DF aided scheme however is readily achieved by replacing $\mathbf{H}$ by $\mathbf{H}_1$ and $\mathbf{x}$ by $\mathbf{r}$ in the subsequent equations.

The ML detection of the transmitted signal vector given in Equation (3) can be formulated as

$$\hat{\mathbf{s}} = \arg\max_{\check{\mathbf{s}} \in \mathcal{S}} P(\check{\mathbf{s}}|\mathbf{x}, \mathbf{H}), \tag{7}$$

where $\mathcal{S}$ is the set of potentially transmitted symbol vectors $\mathbf{s}$. Note that in this formulation the super-vector $\mathbf{s}$ is detected, rather than only the subvector $\boldsymbol{s}_{\Delta+1}$ of interest. In the absence of any a priori knowledge about the transmitted data, Equation (7) may be re-written as

$$\hat{\mathbf{s}} = \arg\min_{\check{\mathbf{s}} \in \mathcal{S}} \{||\check{\mathbf{x}} - \mathbf{H}\check{\mathbf{s}}||^2\}. \tag{8}$$

Let us assume for the derivation of the algorithm that the channel matrix $\mathbf{H}$ is real-valued and that the transmitted signal is Binary Phase Shift Keying (BPSK) modulated. It was shown in [1] that the solution to the problem defined by Equation (8) is identical to solving

$$\hat{\mathbf{s}} = \arg\min_{\check{\mathbf{s}} \in \mathcal{S}} ||\mathbf{U}(\check{\mathbf{s}} - \hat{\mathbf{s}}_{MMSE})||^2, \tag{9}$$

where the upper triangular matrix $\mathbf{U}$ is defined by

$$\mathbf{U}^H\mathbf{U} = \mathbf{H}^H\mathbf{H} + \sigma^2\mathbf{I}, \tag{10}$$

while

$$\hat{\mathbf{s}}_{MMSE} = (\mathbf{H}^H\mathbf{H} + \sigma^2\mathbf{I})^{-1}\mathbf{H}^H\mathbf{x}. \tag{11}$$

Let us now first define $N_s = Q(M+L-1)$ which is number of symbols in $\mathbf{s}$ considered by the OHRSA. Exploiting the fact that the matrix $\mathbf{U}$ has an upper triangular structure, it can be shown that the objective function used for the detection of the transmitted symbol vector $\check{\mathbf{s}}$ may be written as [1]

$$\begin{aligned} J(\check{\mathbf{s}}) &= ||\mathbf{U}(\check{\mathbf{s}} - \hat{\mathbf{s}}_{MMSE})||^2 && (12) \\ &= (\check{\mathbf{s}} - \hat{\mathbf{s}}_{MMSE})^H\mathbf{U}^H\mathbf{U}(\check{\mathbf{s}} - \hat{\mathbf{s}}_{MMSE}) && (13) \\ &= \sum_i^{N_s} |\sum_{j=i}^{N_s} u_{ij}(\check{s}_j - \hat{s}_{j,MMSE})|^2 && (14) \\ &= \sum_i \phi_i(\check{\mathbf{s}}_i), && (15) \end{aligned}$$

where $\phi(\check{\mathbf{s}}_i)$ may be expressed as [1]

$$\begin{aligned} \phi(\check{\mathbf{s}}_i) &= |u_{ii}(\check{s}_i - \hat{s}_{j,MMSE}) \\ &\quad \underbrace{+ \sum_{j=i+1}^{N_s} u_{ij}(\check{s}_i - \hat{s}_{j,MMSE})|^2}_{a_i}, \end{aligned} \tag{16}$$

and where the second term of Equation (16) is independent of the specific symbol's value of $\check{s}_i$. The cost function given in Equation (15) may now be re-written in a recursive manner as

$$J_i(\check{\mathbf{s}}_i) = J_{i+1}(\mathbf{s}_{i+1}) + \phi(\mathbf{s}_i), \quad i = N_s - 1, \ldots 1, \tag{17}$$

where we have $J(\check{s}_{N_s}) = |u_{N_sN_s)(\check{s}_{N_s} - \hat{s}_{N_s,MMSE})}|^2$. The cost function has the essential property that [1]

$$J(\mathbf{s}) = J_1(\mathbf{s}_1) > J_2(\mathbf{s}_2) > \cdots > J_{N_s}(s_{N_s}) > 0. \tag{18}$$

Due to the fact that the cost function $J_i(\check{\mathbf{s}}_i)$ only depends on $\{\check{s}_i, \ldots, \check{s}_{N_s}\}$, we introduce the notation

$$J_i(\check{\mathbf{s}}_i) = J_i([\check{s}_i, \ldots, \check{s}_{N_s}]^T) = J_i([\check{s}_i \ \check{\mathbf{s}}_{i+1}]^T). \tag{19}$$

This property facilitates an effective low complexity search, which is outlined in detail in [1]. To ensure that the algorithm operates efficiently, it is advisable to reorder the channel matrix first in increasing order according to the norm of the columns. This will result in a 'best-first' detection strategy, as outlined in [2].

Consider now a simple candidate system supporting $K = 2$ MSs, employing $N_{Tx} = 1$ AE each, a $L = 2$-path channel and a BS configuration given as $M = 2$, $\Delta = 1$ and $N_{Rx} = 2$. This system configuration results in a $(N_{Rx}M \times KN_{Tx}(M+L-1))$-dimensional channel matrix constructed according to Equation (3). The $KN_{Tx}(M+L-1)$-element signal vector contains $(M+L-1)$ number of consecutively transmitted vectors $\boldsymbol{s}$, each hosting KN_{Tx} number of elements. The (MN_{Rx})-element channel output $\mathbf{x}$ is given as the product of the channel matrix $\mathbf{H}$ and the transmitted symbol vector $\mathbf{s}$ plus the AWGN. The characteristic quantities of such a system are given for example as

$$\mathbf{H} = \begin{bmatrix} 0.45 & 0.16 & 0.89 & 0.47 & 0 & 0 \\ 0.39 & 0.30 & 0.92 & 0.40 & 0 & 0 \\ 0 & 0 & 0.45 & 0.16 & 0.89 & 0.47 \\ 0 & 0 & 0.39 & 0.30 & 0.92 & 0.40 \end{bmatrix}$$

$$\mathbf{x} = \begin{bmatrix} -1.37 \\ -1.20 \\ 0.04 \\ 0.44 \end{bmatrix} \quad \text{and} \quad \mathbf{s} = \begin{bmatrix} +1 \\ -1 \\ -1 \\ +1 \\ +1 \\ -1 \end{bmatrix}, \tag{20}$$

This corresponds to a scenario, where the first MS's signal is received at 6 dB higher power than the signal of the second MS.

As mentioned earlier, the convergence of the algorithm can be improved by reordering the columns of the channel matrix $\mathbf{H}$, so that the columns of the reordered channel matrix have increasing power [2] [1]. Commencing the algorithm now by reordering the channel matrix of Equation (20) yields $\mathbf{H}^{(o)}$, where the superscript $^{(o)}$ stands for ordered.

$$\mathbf{H}^{(o)} = \begin{bmatrix} 0.16 & 0.45 & 0 & 0.47 & 0 & 0.89 \\ 0.30 & 0.39 & 0 & 0.40 & 0 & 0.92 \\ 0 & 0 & 0.47 & 0.16 & 0.89 & 0.45 \\ 0 & 0 & 0.40 & 0.30 & 0.92 & 0.39 \end{bmatrix}. \tag{21}$$

It may be readily shown that the corresponding upper triangular decomposition of $\mathbf{H}$ into $\mathbf{U}^{(o)}$ and the required MMSE solution for the ordered system are given as

$$\mathbf{U}^{(o)} = \begin{bmatrix} 0.42 & 0.44 & 0 & 0.46 & 0 & 0.99 \\ 0 & 0.47 & 0 & 0.35 & 0 & 0.69 \\ 0 & 0 & 0.67 & 0.29 & 1.19 & 0.55 \\ 0 & 0 & 0 & 0.38 & 0.19 & 0.33 \\ 0 & 0 & 0 & 0 & 0.52 & 0.06 \\ 0 & 0 & 0 & 0 & 0 & 0.45 \end{bmatrix} \tag{22}$$

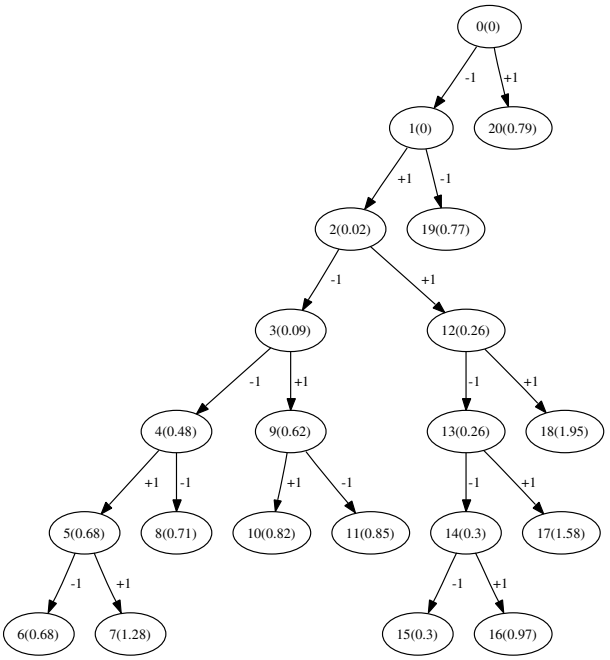

Fig. 1. Example of a search tree formed by the OHRSA based STE in a scenario employing BPSK modulation, $N_{Rx} = 2, M = 2$, $\Delta = 1$, $L = 2$, $K = 2$ and $N_{Tx} = 1$ and encountering $E_{b/N_0} = 12$ dB. The exact received signal vector $\mathbf{x}$, the channel matrix $\mathbf{H}$ and the transmitted sequence $\mathbf{s}$ are given in Equation (20). The labels indicate the search node index, while the value of the costfunction of Equation (17) is given in brackets.

and

$$\hat{\mathbf{s}}^{(o)}_{MMSE} = [-0.11 \ -0.61 \ 0.10 \ -0.12 \ 0.69 \ -1.01]^T. \tag{23}$$

Note that since both the system matrix and the transmitted signal are real-valued, the imaginary part of the received sequence may be omitted and the MMSE solution is also real-valued. The algorithm commences at node 0 of Figure 1 by evaluating the cost function of the hypothetical solutions $\check{s}^{(o)}_{N_s} = \check{s}^{(o)}_6$ associated with the ordered channel matrix of Equation (21), according to Equation (17), which yields

$$\begin{aligned} J_6(\check{s}_6)^{(o)} &= |u^{(o)}_{66}(\check{s}^{(o)}_6 - \hat{s}^{(o)}_{6,MMSE})|^2 \\ J_6(\check{s}^{(o)}_6 = +1) &= |.45 \cdot (+1 + 1.01)|^2 = 0.79 \\ J_6(\check{s}^{(o)}_6 = -1) &= |.45 \cdot (-1 + 1.01)|^2 = 0.00. \end{aligned}$$

The two values $J_6(\check{s}^{(o)}_6)$ can be seen at the second hierarchical level of Figure 1 as nodes 1 and 20 together with the associated hypothetical BPSK solutions indicated along the branches. Based on the two cost function values seen within node 1 and 20 we select node 1, since it has a value of $J_6(\check{s}^{(o)}_6 = -1) = 0.0$, which is the lower cost function value. The associated symbol value is $\check{s}^{(o)}_6 = -1$. In the next step of the algorithm we proceed from node 1 of Figure 1 by calculating the cost function of Equation (17) for the next two potential values of $\check{s}^{(o)}_5 = \pm 1$ as follows:

$$\begin{aligned} a_5 &= \textstyle\sum_{j=6}^{6} u^{(o)}_{5j} \cdot (\check{s}^{(o)}_j - \hat{s}^{(o)}_{j,MMSE}) \\ &= 0.06 \cdot (-1 + 1.01) = 0.00 \\ J_5([\check{s}^{(o)}_5 \ -1]^T) &= |a_5 + u^{(o)}_{55}(\check{s}_5 - \hat{s}^{(o)}_{5,MMSE})|^2 \\ J_5([+1 \ -1]^T) &= |0.00 + .52 \cdot (+1 - .68)|^2 = 0.02 \\ J_5([-1 \ -1]^T) &= |0.00 + .52 \cdot (-1 - .68)|^2 = 0.77. \end{aligned}$$

The resultant two values for $J_5(\check{\mathbf{s}}^{(o)}_5)$ are associated with node 2 and 19, respectively, which are seen at the third hierarchical level of Figure 1. The node from which the algorithm is further evolving

is node 2, where the associated symbol is $\check{s}_5^{(o)} = +1$, which has a lower cost function value than node 19.

The value of $\check{\mathbf{s}}_5^{(o)} = [+1 \ -1]^T$ is now used for the calculation of the cost function values of Equation (17) associated with $\check{\mathbf{s}}_4^{(o)}$. The cost function values $J_4(\check{\mathbf{s}}_4^{(o)})$ are illustrated at the fourth hierarchical level of Figure 1 within node 3 and 12. Repeating this procedure will result in the calculation of the cost function value of $J_3(\check{\mathbf{s}}_3^{(o)})$ provided within node 4 and 9 at the fifth hierarchical level of Figure 1, the calculation of $J_2(\check{\mathbf{s}}_2^{(o)})$ given in node 5 and 8 at the sixth hierarchical level of Figure 1 and finally $J_1(\check{\mathbf{s}}_1^{(o)})$ given in node 6 and 7 at the seventh and last hierarchical level of Figure 1.

Upon arriving at $J_1(\check{\mathbf{s}}_1^{(o)})$ at the bottom of the graph, we have calculated the first potential solution of our optimization problem described by Equation (7), which is constituted by the left-most branch of the search tree illustrated in Figure 1. This potential solution is given by $\check{\mathbf{s}}^{(o)} = [-1 \ +1 \ -1 \ -1 \ +1 \ -1]^T$.

The recursive optimization continues from the bottom (node 6) to the top of the tree of Figure 1 with the objective of finding the specific branch terminating at the bottom of the search tree (hierarchical level 6) while having the minimum costfunction value. The symbol vector $\mathbf{s}$ associated with this branch constitutes the ML solution. Considering now the flipping of symbol $\check{s}_1^{(o)}$ or $\check{s}_2^{(o)}$ at hierarchical level 5 or 6 is not beneficial, since the cost function associated with these changes would result in a higher value, namely 1.28 and 0.71, than the cost function of 0.68 at node 6. Hence, if these tentative branches would be pursued to the bottom of the tree, it would ultimately result in an increased cost function value as a consequence of the ordering property outlined in Equation (18).

When the recursive process initiated at node 6 arrives at node 3, however, it can be seen that changing the value of $\check{s}_4^{(o)}$ from -1 to $+1$ results in a cost function value of 0.62 at node 3 which is lower than the cost function value of 0.68 recorded at node 6. Pursuing the path from node 9 further down the tree will however again result in a cost function value that is higher than that of node 6. The corresponding branch is therefore not pursued further.

Returning to the most-left branch and changing the value of $\check{s}_4^{(o)}$ from -1 to $+1$, results in a cost function value of 0.26, which is lower than that of node 6 and the corresponding path is therefore pursued further through nodes 13 and 14. Ultimately, this results in two new branches through nodes 12 , 13, 14 and 15 as well as 12, 13, 14 and 16 terminating at $\check{\mathbf{s}}_1^{(o)}$, which constitute additional potential solutions for $\mathbf{s}^{(o)}$. Pursuing this path from node 15 and 16 backwards, returning to the most-left branch and moving recursively up to node 0 will result in no further branches terminating at the bottom of the tree.

The desired solution is described by the specific branch terminating at the bottom of the search tree and having the lowest cost function value. Again, the associated symbol sequence is given by

$$\check{\mathbf{s}}^{(o)} = [-1 \ -1 \ -1 \ +1 \ +1 \ -1]^T,$$

which can be obtained by tracing the branch back from node 15 to node 0. By contrast, the identically ordered MMSE solution is given by

$$\hat{\mathbf{s}}_{MMSE}^{(o)} = [-1 \ -1 \ +1 \ -1 \ +1 \ -1]^T.$$

The corresponding solutions for reversed ordering are then given by

$$\begin{aligned} \check{\mathbf{s}} &= [-1 \ -1 \ \underbrace{-1 \ +1}_{\boldsymbol{s}_{\Delta+1}} \ +1 \ -1]^T \\ \hat{\mathbf{s}}_{MMSE} &= [-1 \ -1 \ \underbrace{-1 \ -1}_{\boldsymbol{s}_{\Delta+1}} \ +1 \ +1]^T \ , \end{aligned}$$

which highlights the decision errors made by the MMSE detector. The fact, that only a subset of the detector outputs is actually of interest, namely the subvector $\boldsymbol{s}_{\Delta+1}$ of $\mathbf{s}$ is a major difference between the OHRSA applied to the non-dispersive OFDM subchannels in [1] and the wideband scenarios considered in this treatise.

Following the procedure outlined in [1], the presented OHRSA readily may be extended to account for complex-valued channel matrices and higher order modulation schemes.

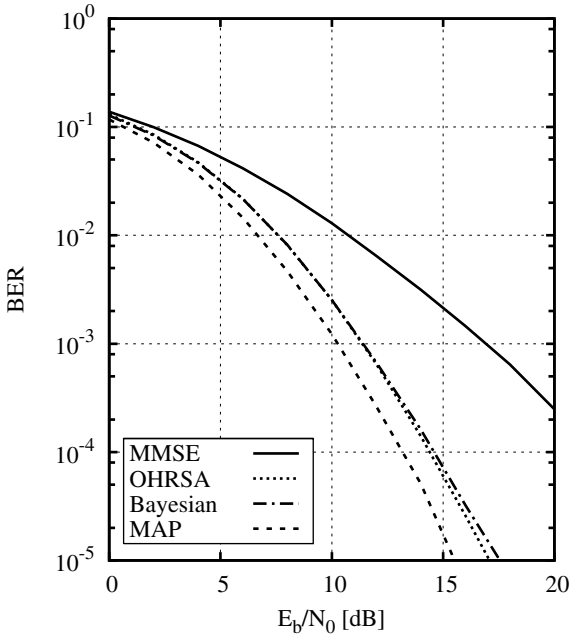

Fig. 2. BER versus E_b/N_0 for a scenario supporting $K = 1$ user employing $N_{Tx} = 2$ transmit AEs, a two-path equal-power block-fading channel, a BS equipped with $N_{Rx} = 2$, $M = 2$, $\Delta = 1$ and perfect channel knowledge. BPSK modulation was considered.

III-A. Results

In order to benchmark the proposed algorithm against conventional DF-STEs proposed in the literature [6] a low-complexity system consisting of $K = 1$ MS benefiting from $N_{Tx} = 2$ number of transmit antennas and communicating over a channel modelled by two equal-power independently faded path. The signal was assumed to be BPSK modulated and the BS employed $N_{Rx} = 2$ receive antennas as well as a DF aided STE in conjunction with $M = 2$, $\Delta = 1$ and $N = 1$. The fading envelope was assumed to be constant during an entire transmission burst and no channel coding was considered.

It can be seen from Figure 2 that the OHRSA indeed approaches the performance bound constituted by the Bayesian DF-STE and clearly outperforms the MMSE-based STE. The performance discrepancy recorded in comparison to the Maximum A-Posteriori (MAP) STE might be closed by considering a higher decision delay in the STE.

Let us now extend the system to 4QAM modulated signals, a BS benefiting from $N_{Rx} = 4$ AEs, which supports various

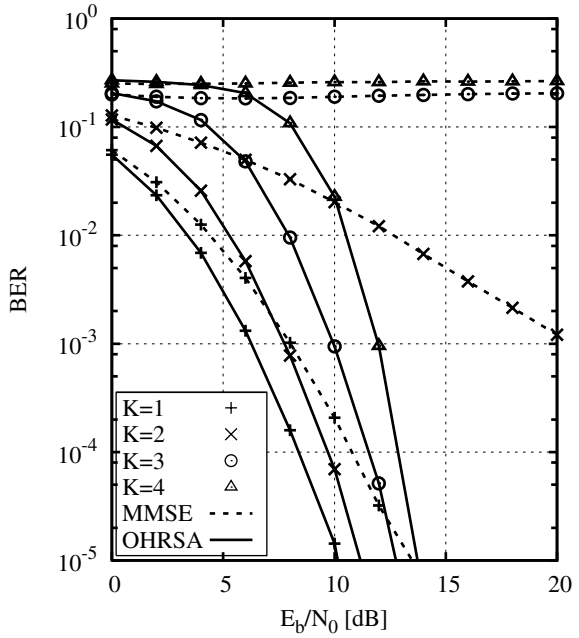

Fig. 3. BER versus E_b/N_0 for a scenario supporting K number of users, each employing $N_{Tx} = 2$ transmit AEs, a two-path equal-power block-fading channel, a BS associated with $N_{Rx} = 4$, $M = 2$, $\Delta = 1$ and perfect channel knowledge. 4QAM transmissions were considered.

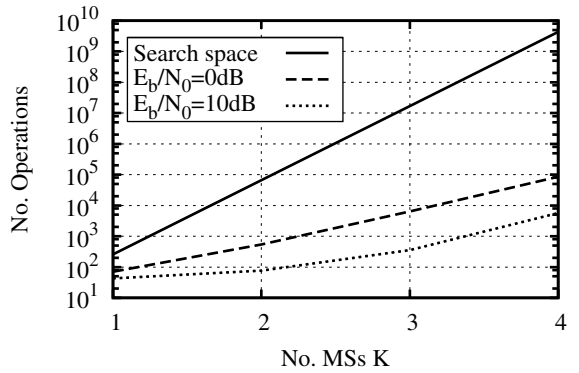

Fig. 4. The number of combined addition and multiplication operations required for the detection of a single bit by the system used for generating Figure 3.

number of MSs K, while keeping the other system parameters as $M = 2$, $\Delta = 1$ and $N = 1$. For this system the classic Bayesian and MAP STE benchmarker are excessively complex, hence only the OHRSA and the MMSE DF-STE are considered. In Figure 3, which shows the attainable average BER versus E_b/N_0 performance for different numbers of MSs it can be observed, that the OHRSA is capable of detecting all MSs' signals, even in heavily overloaded systems, whereas the MMSE STE falters. The complexity required for the detection of the signals associated with Figure 3 is shown in Figure 4. The curve labeled as 'Search Space' indicates the number of possible transmitted bit sequences in the search space, whereas the other curves show the number of operations (multiplications plus additions) required for the evaluation of the cost function given in Equation (15) for the detection of a single bit. The graph clearly indicates that the complexity of the OHRSA is several magnitudes lower than the complexity associated with a full ML detector. It can also be seen that for a higher SNR the number of operations imposed is lower than that required as lower SNRs.

IV. TRUNCATED SEARCH

In contrast to the application of the OHRSA for the detection of the narrowband OFDM subcarriers, the detection of all symbols in $\mathbf{s}$ is not required in the context of wideband systems, since we mentioned earlier that we are only interested in the detection of the subvector $\boldsymbol{s}_{\Delta+1}$.

An attractive way of exploiting this phenomenon is to arrange the columns of the channel matrix $\mathbf{H}$ not only according to the squared norm of the columns as suggested in [1], but also ensuring that the columns of specific interest appear at the end of the ordered channel matrix $\mathbf{H}^{(o)}$. In other words, we try to ensure that the symbols associated with $\boldsymbol{s}_{\Delta+1}$ appear at the top of the search tree and are therefore detected first.

The corresponding reordering scheme can be divided into two steps as follows:

1) Set the last Q number of columns of the channel matrix given by
$$(\mathbf{H})_i \; i \; \in \; [\Delta \cdot Q + 1, (\Delta + 1) \cdot Q]$$
to the columns arranged according to their power. This ensures that the symbols of interest are detected first according to the squared norm of the associated columns. The associated symbols appear in the top section of the search tree.
2) Set the remaining columns of the channel matrix ordered according to the squared norm of the columns to the remaining columns of the channel matrix, again, arranged according to their squared norm.

From a physical point of view the columns with very low squared norm may contribute very little to the final cost function value. This yields, that the search tree is subject to a very fine branching at its bottom levels which has little influence on the final cost function value and increases the complexity because each of these branches has to be evaluated. Due to the fact, that the desired symbols appear now in the top section of the search tree, a certain number of levels at the bottom of the tree might be neglected in order to avoid the evaluation of the cost function associated with the fine branching.

The recursive cost function of Equation (17) can then be rewritten as

$$J_i(\check{s}_i) = J_{i+1}(s_{i+1}) + \phi(s_i), \; i = N_s - 1, \ldots, N_{trunc} + 1, \quad (24)$$

where N_{trunc} indicates the number of layers of the search tree that have been discarded. Note however that truncation will always result in performance degradation, because even though we are not interested in the final decision concerning some of the symbols, they still mildly influence the channel's output vector $\mathbf{x}$ and the cost function as it becomes explicit from Equation (9). Under certain circumstances, however, when the power associated with these symbols is very low (the associated column of the channel matrix has a low squared norm), their influence becomes marginal and might be neglected.

IV-A. Results

The effect of truncating the search tree has first been investigated for the same system as the one studied in Figure 3. The number of operations shown in Table I was recorded for E_b/N_0=10 dB and the associated performance degradation was less than 0.7 dB.

	$K=1$ $N_{trunc}=2$	$K=2$ $N_{trunc}=4$	$K=3$ $N_{trunc}=4$
Full	44	77	353
Trunc.	27	44	122

TABLE I

NUMBER OF OPERATIONS REQUIRED FOR THE DETECTION OF ONE BIT AT E_b/N_0 =10 DB ASSOCIATED WITH THE SYSTEM USED FOR GENERATING FIGURE 3 IF TRUNCATION IS USED.

	$K=1$ $N_{trunc}=4$	$K=2$ $N_{trunc}=8$
Full	254	$7.1 \cdot 10^4$
Trunc.	60	193

TABLE II

NUMBER OF OPERATIONS REQUIRED FOR THE DETECTION OF ONE BIT AT E_b/N_0 =10 DB ASSOCIATED WITH THE SYSTEM USED FOR GENERATING FIGURE 5 IF TRUNCATION IS USED.

Due to lack of space the corresponding BER curves are not included. It is worth mentioning that the two-path equal-power model channel may be considered to correspond to the worst-case scenario, because the difference in squared norm between the columns of the channel matrix associated with the desired and the undesired symbols is not dramatic.

Let us therefore consider a more optimistic propagation scenario having four equal-power paths and a DF-STE associated with $M = 4$, $\Delta = 3$, $N = 3$ and $N_{Rx} = 4$ receive antennas. Each user employed $N_{Tx} = 2$ transmit AEs and the channel code employed was a half-rate punctured turbo-code [4] which was operating on the hard-decision output of the DF-STE. In Table II the complexity reduction achieved as a benefit of the above-mentioned truncation procedure is summarized and the associated BER performance is shown in Figure 5. It can be observed that the truncation technique in this scenario provides a significant complexity reduction which is of several orders of magnitudes attained at the cost of little performance degradation. The associated high number of operations required for the conventional OHRSA assisted DF-STE is due to the fact that the low power associated with some columns of the channel matrix results in numerous extra branches at the bottom of the search tree all of which have to be considered by the algorithm. It is exactly this set of low-power branches, which can be truncated without any significant loss of performance. The higher difference in squared norm compared to the two-path system is caused by the Toeplitz structure of the channel matrix $\mathbf{H}$, which is the characteristic of STEs.

V. CONCLUSION

A novel DF aided reduced complexity ML detector has been proposed for employment in single-carrier wideband scenarios . The detector was based on the recently contrived OHRSA algorithm [1], which has been further developed for employment in a single-carrier STE. It was shown that the proposed receiver struture substantially outperforms the linear benchmarker based on the MMSE criterion. Furthermore, a complexity reduction scheme based on truncating the search tree has been proposed, which accommodates the specific properties of the associated propagation channel. The proposed modification of the OHRSA complements

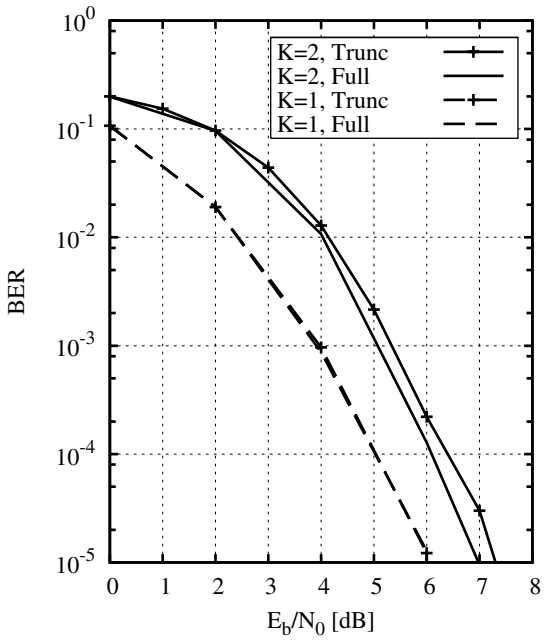

Fig. 5. BER versus E_b/N_0 for a scenario supporting K number of users, each employing $N_{Tx} = 2$ transmit AEs, a four-path equal-power block-fading channel, a BS associated with $N_{Rx} = 4$, $M = 4$, $\Delta = 3$ and perfect channel knowledge. 4QAM transmissions and a half-rate turbo code were considered.

the DF-STE in a sense, that the symbols associated with the post-cursor of the CIR can be combatted by the DF structure, whereas the low-power pre-cursor of the CIR might be neglected for the sake of reducing the complexity of the OHRSA aided STE by truncating the search tree.

VI. REFERENCES

[1] J. Akhtman and L. Hanzo, "Reduced-complexity maximum-likelihood detection in multiple-antenna-aided multicarrier systems," in *Proceedings of 5th Int'l Workshop on Multi-Carrier Spread Spectrum (in press)*, (Oberpfaffenhofen, Germany), 2005.

[2] L. Hanzo, M. Münster, B. Choi, and T. Keller, *OFDM and MC-CDMA for Broadcasting Multi-User Communications, WLANs and Broadcasting*. John Wiley and IEEE Press, July 2003.

[3] B. Hassibi and H. Vikalo, "On the sphere-decoding algorithm I. Expected complexity," *Signal Processing, IEEE Transactions on [see also Acoustics, Speech, and Signal Processing, IEEE Transactions on]*, vol. 53, pp. 2806–2818, 2005.

[4] L. Hanzo, C. H. Wong, and M. S. Yee, *Adaptive Wireless Transceivers: Turbo-Coded, Turbo-Equalized and Space-Time Coded TDMA, CDMA, and OFDM Systems*. John Wiley and IEEE Press, Feb. 2002.

[5] S. Chen, B. Mulgrew, E.-S. Chng, and G. J. Gibson, "Space translation properties and the minimum-BER linear-combiner DFE," *IEE Proceedings on Communications*, vol. 145, pp. 316–322, October 1998.

[6] A. Wolfgang, S. Chen, and L. Hanzo, "Radial basis function network assisted wide-band beamforming," *Vehicular Technology Conference*, pp. 266–270, Sept. 2004.